UCSF
UC San Francisco Previously Published Works

Title

Comorbid neuropathological diagnoses in early versus late-onset Alzheimer's disease

Permalink

https://escholarship.org/uc/item/9f03x2sw

Journal

Brain, 144(7)

ISSN

0006-8950

Authors

Spina, Salvatore
La Joie, Renaud
Petersen, Cathrine
et al.

Publication Date

2021-08-17

DOI

10.1093/brain/awab099

Peer reviewed

BRAIN
ORIGINAL ARTICLE

Comorbid neuropathological diagnoses in early versus late-onset Alzheimer's disease

Salvatore Spina,[1,†] Renaud La Joie,[1,†] Cathrine Petersen,[1] Amber L. Nolan,[1]
Deion Cuevas,[1] Celica Cosme,[1] Mackenzie Hepker,[1] Ji-Hye Hwang,[1]
Zachary A. Miller,[1] Eric J. Huang,[2] Anna M. Karydas,[1] Harli Grant,[1] Adam L. Boxer,[1]
Maria Luisa Gorno-Tempini,[1] Howard J. Rosen,[1] Joel H. Kramer,[1] Bruce L. Miller,[1]
William W. Seeley,[1,2] Gil D. Rabinovici[1,3] and Lea T. Grinberg[1,2]

†These authors contributed equally to this work.

Co-pathologies play an important role in the expression of the Alzheimer's disease clinical phenotype and may influence treatment efficacy. Early-onset Alzheimer's disease, defined as manifesting before age 65, is viewed as a relatively pure form of Alzheimer's disease with a more homogeneous neuropathological substrate.

We sought to compare the frequency of common neuropathological diagnoses in a consecutive autopsy series of 96 patients with early-onset Alzheimer's disease (median age of onset = 55 years, 44 females) and 48 with late-onset Alzheimer's disease (median age of onset = 73 years, 14 females). The UCSF Neurodegenerative Disease Brain Bank database was reviewed to identify patients with a primary pathological diagnosis of Alzheimer's disease. Prevalence and stage of Lewy body disease, limbic age-related TDP-43 encephalopathy (LATE), argyrophilic grain disease, hippocampal sclerosis, cerebral amyloid angiopathy, and vascular brain injury were compared between the two cohorts.

We found at least one non-Alzheimer's disease pathological diagnosis in 98% of patients with early-onset Alzheimer's disease (versus 100% of late onset), and the number of comorbid diagnoses per patient was lower in early-onset than in late-onset Alzheimer's disease (median = 2 versus 3, Mann-Whitney Z = 3.00, P = 0.002). Lewy body disease and cerebral amyloid angiopathy were common in both early and late onset Alzheimer's disease (cerebral amyloid angiopathy: 86% versus 79%, Fisher exact P = 0.33; Lewy body disease: 49% versus 42%, P = 0.48, respectively), although amygdala-predominant Lewy body disease was more common in early than late onset Alzheimer's disease (22% versus 6%, P = 0.02). In contrast, LATE (35% versus 8%, P < 0.001), hippocampal sclerosis (15% versus 3%, P = 0.02), argyrophilic grain disease (58% versus 41%, P = 0.052), and vascular brain injury (65% versus 39%, P = 0.004) were more common in late than in early onset Alzheimer's disease, respectively. The number of co-pathologies predicted worse cognitive performance at the time of death on Mini-Mental State Examination [1.4 points/pathology (95% confidence interval, CI –2.5 to –0.2) and Clinical Dementia Rating-Sum of Boxes (1.15 point/pathology, 95% CI 0.45 to 1.84)], across early and late onset cohorts. The effect of sex on the number of co-pathologies was not significant (P = 0.17). Prevalence of at least one *APOE* ε4 allele was similar across the two cohorts (52% and 54%) and was associated with a greater number of co-pathologies (+ 0.40, 95% CI 0.01 to 0.79, P = 0.047), independent of age of symptom onset, sex, and disease duration. Females showed higher density of neurofibrillary tangles compared to males, controlling for age of onset, *APOE* ε4, and disease duration.

Our findings suggest that non-Alzheimer's disease pathological diagnoses play an important role in the clinical phenotype of early onset Alzheimer's disease with potentially significant implications for clinical practice and clinical trials design.

1 Department of Neurology, Memory and Aging Center, Weill Institute for Neurosciences, University of California, San Francisco, San Francisco, CA 94158, USA
2 Department of Pathology, University of California, San Francisco, San Francisco, CA 94143, USA
3 Department of Radiology and Biomedical Imaging, University of California, San Francisco, San Francisco, CA 94143, USA

Correspondence to: Salvatore Spina
University of California, San Francisco (UCSF)
Memory and Aging Center, 675 Nelson Rising Lane
Suite 190, San Francisco, CA 94158, USA
E-mail: salvatore.spina@ucsf.edu

Introduction

The coexistence of multiple proteinopathies and vascular brain injury is a common finding in the brains of the elderly, the number of distinct pathological entities being strongly correlated with age and genetic factors, such as the *APOE* genotype.[1–3] While numerous proposed mechanisms of mutual induction support the biological interaction of some of these proteinopathies, the occurrence of other co-pathologies appears to be a time-dependent phenomenon, with the likelihood of accumulating more distinct types of brain pathology reflecting longer survival.[4] Alzheimer's disease neuropathological changes are frequently associated with a high prevalence of coexistent Lewy body disease (LBD) and/or TDP-43 proteinopathy, which influence the clinical phenotype.[5–9] While prior studies have begun elucidating the prevalence of coexisting pathology in Alzheimer's disease, differences in the number and type of co-pathologies between sporadic early-onset Alzheimer's disease (EOAD) and late-onset Alzheimer's disease (LOAD) patients are less well characterized.[2,3] Sporadic EOAD defines the small proportion of patients with Alzheimer's disease whose clinical onset occurs before the age of 65 years, in the absence of Alzheimer's disease pathogenic mutations. Despite the historical and arbitrary age-based classification,[10] and in spite of sharing the same hallmark neuropathological features, amyloid-β plaques and tau-immunoreactive neurofibrillary tangles (NFT), EOAD and LOAD are commonly referred to as potentially diverging clinicopathological entities on the basis of differences in the phenotypic presentation and genetic predisposition.[11] Because of the onset in young age, EOAD represents the ideal model to contrast the two hypotheses of the mutual induction of distinct co-pathologies versus the age-dependent model leading to co-pathology accumulation in Alzheimer's disease. Here, we report the frequency and severity of coexisting co-pathologies in a cohort of consecutive patients with a primary neuropathological diagnosis of Alzheimer's disease, and at the age of onset of cognitive symptoms consistent with either EOAD or LOAD.

Materials and methods

Neuropathological criteria for cases selection

We searched the Neurodegenerative Diseases Brain Bank (NDBB) database of the University of California, San Francisco to identify cases with a primary pathological diagnosis of Alzheimer's disease, assessed by expert neuropathologists (S.S., E.J.H., W.W.S., and L.T.G.) between September 2008 and March 2020. The brains were obtained post-mortem, processed, and 24 anatomical regions were analysed according to the NDBB research protocol, as previously described.[12] Details on the brain regions assessed and histological and immunohistochemical methods are described in the Supplementary material. Of 516 cases, the search returned 190 cases with primary pathological diagnosis of Alzheimer's disease,[13] based on NFT stage,[14] Thal amyloid-β phase,[15] and neuritic plaques frequency assessment.[16] Primary pathological diagnosis is herein defined as the most developed neuropathological entity, which severity and regional distribution are thought to explain the majority of the patient's clinical cognitive and behavioural phenotype. Contributing pathological diagnosis is defined as a coexistent neuropathological entity that is sufficiently developed to likely contribute to the primary clinical phenotype or to additional clinical features that cannot be otherwise attributed to the primary pathological diagnosis. Since the goal of the study was to ascertain the relative frequency of the most common non-Alzheimer's disease neurodegenerative co-pathologies [LBD, limbic age-related TDP-43 encephalopathy (LATE), argyrophilic grain disease (AGD), hippocampal sclerosis (HS), and cerebral amyloid angiopathy (CAA)] among the two cohorts of EOAD and LOAD, 12 cases were excluded because of a co-primary or contributing diagnosis of frontotemporal lobar degeneration.[8,17–19] HS is defined based on modified published criteria, with the additional definition of selective neuronal loss of the hippocampus and subiculum as an estimated loss higher than 90% of the expected regional neuronal population.[20] Efforts were made to differentiate epilepsy-associated and vascular-associated HS, not covered by the beforementioned criteria. Since LATE and HS can occur independently and HS is not always associated with TDP-43 immunoreactivity, LATE and HS were considered distinct pathologies.[21] CAA was added to the total number of non-Alzheimer's disease co-pathologies because its presence is not accounted in the current pathological diagnostic criteria for Alzheimer's disease neuropathological changes, and because of a possible direct impact on cognition independent of CAA-related vascular brain injury or CAA-related neuroinflammation.[13,22] Five cases were excluded because of a co-primary diagnosis of primary lateral sclerosis with TDP-43 inclusions, CAA-related neuroinflammation, chronic traumatic

encephalopathy (CTE, two cases), or vascular brain injury (a case of intraparenchymal haemorrhage), and one additional case was excluded because of contributing traumatic brain injury with diffuse axonal degeneration.[23–25] CAA-related neuroinflammation was excluded because of the subacute neurobehavioural symptoms—partially responsive to immunosuppression—that differentiates this syndrome from the clinical course of the other Alzheimer's disease co-pathologies.[24] This led to the identification of a pathological cohort of 173 cases.

Next, cases were excluded if information pertinent to Alzheimer's disease neuropathological change severity, including Thal phase, Braak stage, and Consortium to Establish a Registry for Alzheimer's Disease (CERAD) neuritic plaque frequency stage were unavailable,[13] which led to the exclusion of 20 additional cases. We also excluded cases lacking cognitive decline and cases with autosomal dominant Alzheimer's disease (see below), resulting in

a final cohort of 144 (93.75% white; 16.2 ± 2.7 years of education). Figure 1 depicts the flow chart of case selection.

Additional neuropathological assessment

LBD staging (Braak 1–6) was assessed through α-synuclein immunohistochemistry according to published criteria.[26] Because of the high prevalence of cases with LBD pathology non-conforming to the Braak criteria and primarily confined to the amygdala and/or limbic brain regions with minimal or no involvement of brainstem and neocortex, an additional category of amygdala-predominant LBD was considered. TDP-43 proteinopathy was assessed as absent, limbic-predominant (LATE-NC stages I and II) or diffuse (LATE-NC stage III) according to published criteria.[8] AGD was assessed as previously described,[27] and staged as absent, limbic-predominant, or diffuse/neocortical. A diagnosis of HS was given to cases with above 90% neuronal loss in CA1/subiculum.[28]
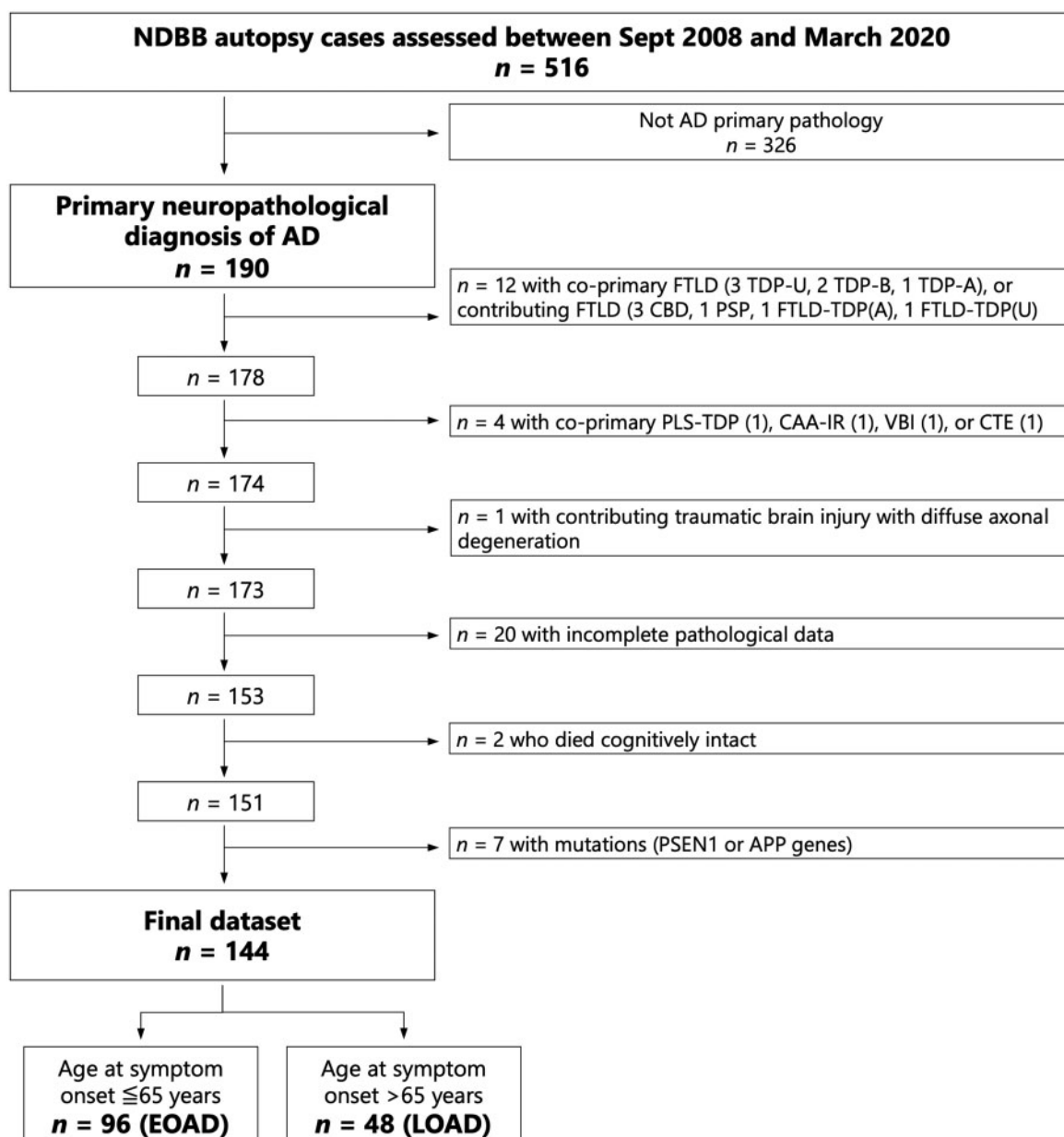

Figure 1 Flow chart of patient selection. AD = Alzheimer's disease; CTE = chronic traumatic encephalopathy; CAA-IR = CAA-related neuroinflammation; CBD = corticobasal degeneration/syndrome; FTLD = frontotemporal lobar degeneration; PLS-TDP = primary lateral sclerosis with TDP-43 inclusions; VBI = vascular brain injury

Vascular brain injury pathology was assessed macroscopically by direct observation of the surfaces of the coronal slabs at the time of autopsy regarding ischaemic and haemorrhagic infarcts, both large and lacunar/small, as previously described.[29] Microinfarcts were instead defined as old areas of regional ischaemia with tissue loss only visible through microscopic assessment, assessed by visual inspection at ×10 magnification of each of the 24 regions of interest. Since no haemorrhages or microbleeds were observed in the final cohort of 144 cases, vascular brain injury pathology was considered present when either macroinfarcts or old microinfarcts were observed, regardless of the regional distribution. White matter rarefaction of presumed vascular origin was not included in this assessment, because the differentiation between a neurodegenerative aetiology of the findings from a purely vascular aetiology is often difficult. CAA semiquantitative rating was carried out using a modified version of a topographic method previously described.[30] A score of 0 meant no amyloid-β immunoreactivity in the leptomeningeal or superficial cortical blood vessels; 'mild' reflected trace to scattered positivity in either the leptomeningeal or the cortical blood vessels; 'moderate' indicated that at least some vessels in the leptomeninges or neocortex had circumferential brightly staining amyloid deposits; and a score of 'severe' corresponded to widespread circumferential amyloid-β positivity in many leptomeningeal and superficial cortical vessels. Ageing-related tau astrogliopathy (ARTAG),[31] including argyrophilic thorny astrocytes in clusters (ATAC) pathology, also known as white matter thorny shaped astrocytes,[32,33] was assessed. Still, its presence was not added to the total number of co-pathologies since data were missing for 36 participants. Presence of contributing CTE was also assessed.[25] Since CTE is linked to exposure to repeated head trauma within a specific environmental setting, this pathology was not added to the total number of co-pathologies to avoid ascertainment bias between the two cohorts. Except for data on ATAC (missing in one case) and ARTAG (missing on 35 cases), only cases ($n = 153$, including 103 with EOAD and 50 with LOAD) for which the full assessment of the aforementioned pathological entities was carried out were included in the study. Taking advantage of data obtained through a previous study,[34] NFT densities were available from the middle frontal gyrus, superior temporal gyrus, primary motor cortex, angular gyrus, and/or CA1/subiculum of 54 EAOD and 23 LOAD patients.

Clinical assessment, genetic screening, and cohort definitions

Clinical information on each of the 153 patients in the pathology dataset was reviewed. All cases had been enrolled during life in longitudinal studies on neurodegenerative dementia at the Memory and Aging Center, UCSF. Information on sex, age at onset, and age at death were collected. Clinical diagnoses were provided by expert behavioural neurologists, according to published criteria.[19,35–42] For this study's purpose, the reported clinical diagnosis for each patient refers to the final best-fit clinical syndromic diagnosis at the latest UCSF clinical assessment. Age at onset was defined as the age of occurrence of the first clinical symptom of Alzheimer's disease as determined by the UCSF clinician based on the patient's clinical history. Patients with age at onset of 65 years or younger were assigned to the EOAD group, while patients with age at onset higher than 65 were assigned to the LOAD group. Age at onset was not available for three participants: two of them died cognitively unimpaired, respectively, at ages 91 and 97 and were excluded from the study; the third subject developed mild cognitive impairment a few years before dying at age 74 and was therefore included in the LOAD group. Genetic analyses were carried out in 137/153 patients as previously described.[43] Genetic

screening for pathogenic mutations in the *APP*, *PSEN1*, *PSEN2*, *C9orf72*, *GRN*, *MAPT*, *FUS*, and *TARDBP* genes were carried out in 133 patients. Two additional patients were only screened for the *C9orf72* pathogenic expansion and two more patients were only screened for mutations in either *C9orf72*, *MAPT* or *GRN*. These studies led to the identification of five carriers of an *APP* mutation and two carriers of a *PSEN1* mutation. These seven patients were excluded from the study. This led to a final dataset of 144 patients, subdivided into an EOAD cohort of 96 patients and a LOAD cohort of 48 participants, whose data were used for the analyses. Clinical progression was assessed using consecutive scores on Mini-Mental State Examination (MMSE) available for 137 patients (382 observations), and Clinical Dementia Rating-Sum of Boxes (CDR-SoB) available for 140 patients (485 observations). *APOE* genotype was available for 91 EOAD and 41 LOAD subjects.

Statistical analyses

Frequency of NFT Braak stages, amyloid-β Thal phases, CAA stages, LBD Braak stages and presence or absence of amygdala-predominant LBD, TDP-43 proteinopathy severity, HS, AGD, ATAC, and ARTAG pathology were compared between the two groups of EOAD and LOAD. The number of co-pathologies is defined by the presence of LBD, TDP-43 proteinopathy, HS, AGD, CAA and/or vascular brain injury. Comparison of ordinal variables (e.g. NFT Braak stage) was carried out using Mann-Whitney tests. Comparison of binarized (presence or absence) measures for any pathological entity between the two groups was assessed using the Fisher's exact test. Chi-square test was used to assess differences in the frequency of LBD subtypes (i.e. absent; conforming to Parkinson's disease Braak stage; or amygdala-predominant only) between groups.

For complementary analyses, age of onset was treated as a continuous variable and we assessed its association with neuropathological measures using Spearman's rho coefficient (for continuous or ordinal measures of neuropathology), Mann-Whitney U-tests (for binary pathology measures), or Kruskal-Wallis tests (for non-ordinal neuropathology categories with more than two levels). For Mann-Whitney tests, we report the results using the common language effect size measure [$U/(n_1 \times n_2)$], representing the probability that a random value from Group 1 is greater than a random value from Group 2, similar to the area under the receiver operating curve.

Separate multiple regression models were used to assess the effect of age of onset, *APOE* ε4, sex, and disease duration on the number of comorbid neuropathological diagnoses or the density of NFT in cortical areas. Logistic regression analyses were used to assess how age of onset, *APOE* ε4 carrier status, sex, and disease duration predicted the presence of each comorbid neuropathological diagnosis. Significance values are reported with a $P < 0.05$, uncorrected for multiple comparisons.

To assess the associations between age of disease onset, number of co-pathologies, and the rate of cognitive and clinical decline, we tested a series of linear mixed effect models using either MMSE or CDR-SoB as the dependent variable. All models included a fixed effect for time until death (in years) and random intercept and slope; the time variable was not centered so that the model intercept indicates the predicted MMSE or CDR-SoB value at time of death. Additional fixed effects were considered including main effects for cohort (EOAD versus LOAD) and number of co-pathologies (0 to 6), and three interactions: time until death × cohort, time until death × number of co-pathologies, and a triple time until death × cohort × number of co-pathologies interaction. For each of the two clinical measures, all 14 potential models (Supplementary Tables 1 and 2) were considered, and the optimal model was chosen based on the minimal Akaike

Information Criterion (AIC) and Bayesian Information Criterion (BIC).

Data availability

All data used in this study are available for review upon request.

Results

Demographics and clinical presentation

Age at onset was 55.2±5.8 (mean ± SD), median = 55, min = 44, max = 65 years in the EOAD group (*n* = 96) and 74.0±5.7 years, median = 73, min = 66, max = 90 in the LOAD group (*n* = 48). Age at death was 66.4±6.6 years in the EOAD group, and 83.0±5.9 years in the LOAD group. Disease duration was longer in the EOAD group (11.2±3.9 years) than in the LOAD group (9.0±3.4 years, t = 3.3, *P* = 0.001, Cohen's *d* = 0.59). Both groups included a majority of males (54% in EOAD, 71% in LOAD, Fisher exact *P* = 0.07). There were no differences between the EOAD and LOAD cohorts in regard to ethnic composition and years of education. In the EOAD group, 57 (59%) patients were diagnosed with amnestic Alzheimer's disease, 11 with posterior cortical atrophy, 11 with logopenic variant primary progressive aphasia, seven with corticobasal syndrome, three with behavioural variant frontotemporal dementia (bvFTD), two with mild cognitive impairment, two with dementia with Lewy bodies (DLB), one with Parkinson's disease dementia, one with unspecified primary progressive aphasia and one with unspecified rapidly progressive dementia. In the LOAD group, 33 (69%) patients were diagnosed with amnestic Alzheimer's disease, five with mild cognitive impairment, three with logopenic variant primary progressive aphasia, two with corticobasal syndrome, one with posterior cortical atrophy, one with behavioural variant frontotemporal dementia, one with DLB, one with traumatic encephalopathy syndrome, and one patient did not meet research diagnostic criteria.

Severity of Alzheimer's disease pathological features is higher in early than late onset Alzheimer's disease

NFT Braak stage (Mann-Whitney U = 2860, Z = 4.32, *P* < 0.001) and amyloid-β Thal phase (U = 2724.5, Z = 3.10, *P* = 0.002) were significantly higher in the EOAD group compared to the LOAD group (Fig. 2A). When Alzheimer's disease pathological stages were correlated with age of onset as a continuous variable within the whole cohort (Supplementary Fig. 1A), we observed significant reduction of NFT Braak stage (rho = –0.3, *P* < 0.001) and Thal phase (rho = –0.30, *P* < 0.001) with age.

Quantitative analyses of NFT density in a subgroup of the cohort showed strong group differences between EOAD and LOAD (Fig. 2B). Compared to LOAD, patients with EOAD had higher NFT density in all investigated cortical areas: middle frontal gyrus (U = 1143.5, Z = 5.81, *P* < 0.001), superior temporal gyrus (U = 968.5, Z = 4.28, *P* < 0.001), primary motor cortex (U = 878.5, Z = 3.60, *P* < 0.001), and angular gyrus (U = 971, Z = 4.51, *P* < 0.001). Differences were milder and did not reach the α < 0.05 significance threshold in the two hippocampal regions examined: CA1 (U = 699.5, Z = 1.20, *P* = 0.23) and subiculum (U = 703.5, Z = 1.40, *P* = 0.16). Results were unchanged when analyses were restricted to cases with Braak stage VI. Similar results were obtained when considering age of onset as a continuous variable (Supplementary Fig. 1B) and in models controlling for sex, *APOE* ε4, and disease duration (Table 1).

Coexistent non-Alzheimer's disease pathologies are common in early-onset Alzheimer's disease

The number of non-Alzheimer's disease coexistent pathologies was significantly higher in the LOAD group compared to the EOAD (median = 3 versus 2, U = 1619, Z = 3.00, *P* = 0.002; Fig. 3A). This relationship was also observed when age of onset was treated as a continuous variable in the whole cohort (rho = –0.26, *P* < 0.001; Fig. 3B), and in a multiple regression model controlling for sex, *APOE* ε4, and disease duration (Table 2).

Coexistent non-Alzheimer's disease pathologies were found in all patients with LOAD (48/48) and in 98% (94/96) of EOAD cases; 69 of these 96 cases had more than one non-Alzheimer's disease co-pathology. Among the 25 EOAD cases with single coexisting pathology, 19 showed coexistent CAA pathology, three coexistent AGD, and three concurrent vascular brain injury. Two non-Alzheimer's disease co-pathologies were observed in 31/96 EOAD patients, three coexistent pathological entities in 26/96 EOAD patients, four in 9/96 patients, five in 2/96 patients, and six non-Alzheimer's disease coexistent pathologies in 1/96 EOAD patients. The overall prevalence of coexistent pathologies in the EOAD group was as follows: CAA 86%, LBD 49%, AGD 41%, vascular brain injuries 39%, TDP-43 proteinopathy 8%, and hippocampal sclerosis 3% (Fig. 4). In the LOAD group, the prevalence of non-Alzheimer's disease co-pathology was as follows: CAA 79%, vascular brain injury 65%, AGD 58%, LBD 42%, TDP-43 35%, and HS 15%. Two subjects in the LOAD group (4%) had concurrent CTE pathology. They both had a history of repetitive head trauma secondary to professional participation in a contact sport.

Cerebral amyloid angiopathy pathology is common in early and late onset Alzheimer's disease

CAA frequency was similar in the EOAD and LOAD groups (86% versus 79%, Fisher exact *P* = 0.33; Fig. 4); no group difference was observed when considering the severity of CAA as an ordinal variable (U = 2360, Z = 0.27, *P* = 0.79). No association was found when considering age of onset as a continuous variable (Supplementary Fig. 2), or using a logistic regression model controlling for sex, *APOE* ε4, and disease duration (Table 3).

Lewy-body pathology is equally prevalent in early and late onset Alzheimer's disease

We found no difference in the presence of α-synuclein co-pathology among the two groups: 47/96 (49%) in EOAD versus 20/48 (42%) in LOAD (Fisher's exact *P* = 0.48, Fig. 4). However, when LBD was assessed as three distinct subtypes (i.e. absent; conforming to Parkinson's disease Braak stage; or amygdala-predominant only), we observed a difference between the EOAD and LOAD groups (χ^2 = 5.75, *P* = 0.056) primarily driven by the higher proportion of amygdala-predominant LBD in EOAD (21/96, 22%) compared to LOAD (3/48, 6%); Fisher's exact *P* = 0.02. Results were consistent when analysing age of onset as a continuous variable (Supplementary Fig. 2), or using a logistic regression model controlling for sex, *APOE* ε4, and disease duration (Table 3).

Frequency and severity of other neuropathological diagnoses in early versus late onset Alzheimer's disease

Coexistent TDP-43 proteinopathy (Fisher's exact *P* < 0.001), hippocampal sclerosis (Fisher's exact *P* = 0.02) and AGD (Fisher's exact *P* = 0.052) were more prevalent in the LOAD group compared to EOAD (Fig. 4). The prevalence of coexistent vascular lesions was
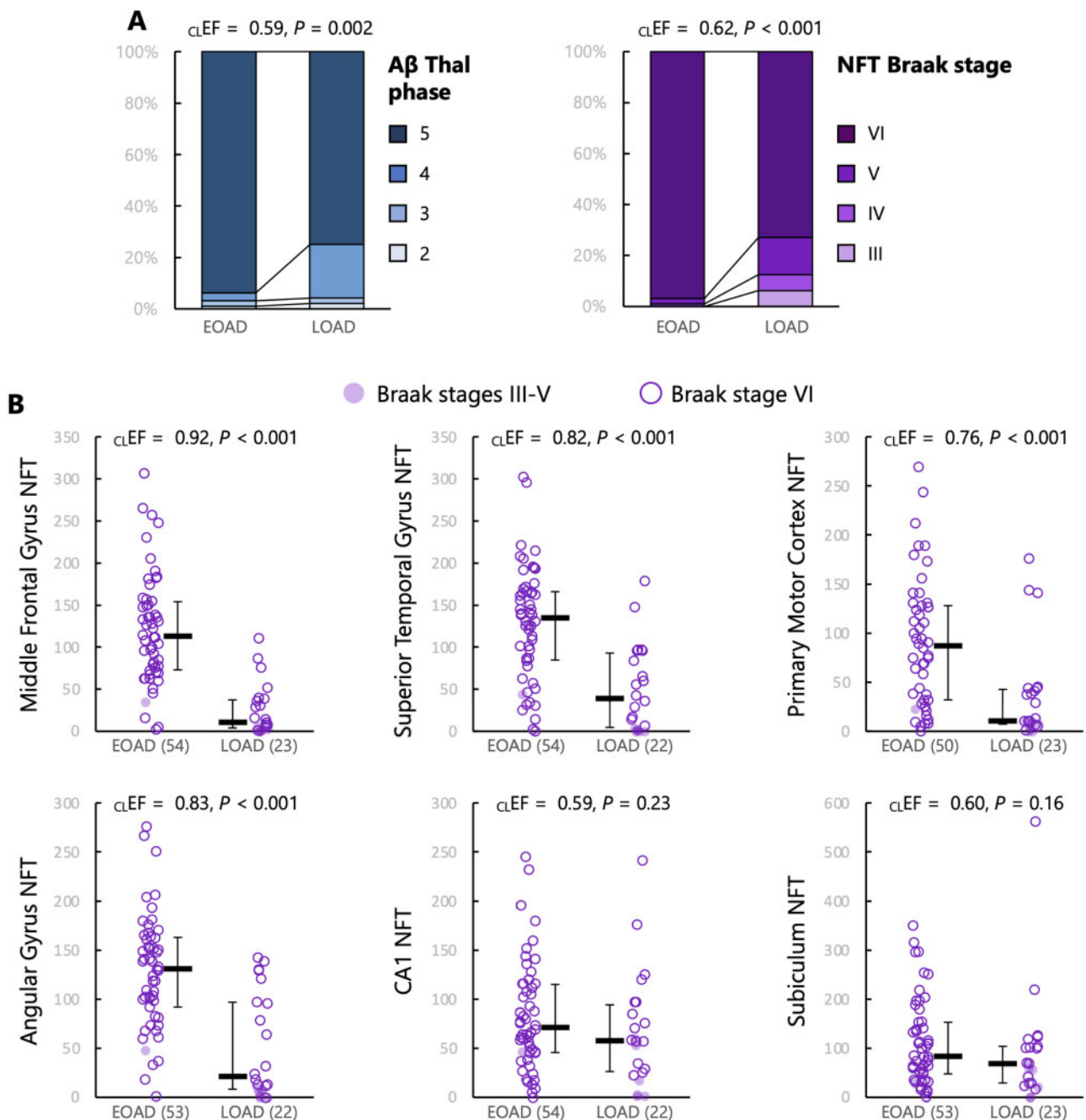
Figure 2 Alzheimer's disease pathology in EOAD and LOAD. (**A**) Ordinal neuropathological scales. (**B**) quantitative analyses of NFT density in six pre-defined regions (density/mm³); bars indicate median and interquartile range. For all variables, Mann-Whitney U-tests were conducted to compare the two groups; common language effect sizes [$_{cL}EF = U / (n_{EOAD} \times n_{LOAD})$] represent the probability that a random value from the EOAD group is greater than a random value from the LOAD group. $n_{EOAD} = 96$ and $n_{LOAD} = 48$, unless otherwise specified. Aβ = amyloid-β.

higher in LOAD than EOAD (65% versus 39%, Fisher's exact $P = 0.004$); *post hoc* analyses showed that both microinfarcts (Fisher's exact $P = 0.004$) and macroscopic (Fisher's exact $P = 0.02$) lesions were more frequent in LOAD than EOAD.

ATAC pathology was more commonly seen in LOAD (21%) than EOAD (14%), though the difference did not reach statistical significance (Fisher's exact $P = 0.33$). ARTAG pathology, not inclusive of ATAC, was significantly more common in LOAD (66%) than EOAD (38%), (Fisher's exact $P = 0.008$).

Similar results were observed when considering age as a continuous variable (Supplementary Fig. 2), or using a logistic regression model controlling for sex, *APOE* ε4, and disease duration (Table 3).

Influence of *APOE* ε4

An *APOE* ε4 allele was found in 47/91 (52%) EOAD subjects and in 22/41 (54%) LOAD patients (Fisher's exact $P = 0.85$). *APOE* ε2 was only present in seven cases (5/91 EOAD, 2/41 LOAD) and was not included as a covariate in subsequent analyses because of low power.

The effect of *APOE* ε4 (coded as *APOE* ε4 carriers versus non-carrier) was assessed on both Alzheimer's neuropathology and comorbid neuropathological diagnosis. *APOE* ε4 status was not associated with amyloid-β Thal phase ($U = 2228.5$, $Z = 0.11$, $P = 0.91$), NFT Braak stage (Mann-Whitney $U = 2156.5$, $Z = 0.77$, $P = 0.44$), or regional NFT

Table 1 Relative impact of age of onset, sex, APOE ε4, and disease duration on the density of neurofibrillary tangles in six cortical regions

NFT density	Middle frontal gyrus	Superior temporal gyrus	Primary motor cortex	Angular gyrus	CA1	Subiculum
n	70	69	66	69	69	68
R² (full model)	0.407	0.376	0.253	0.326	0.210	0.159
Age of onset						
Estimate	–4.49	–3.34	–2.98	–3.23	0.35	0.44
95% CI	–6.01 to –2.97	–4.90 to –1.77	–4.60 to –1.36	–4.71 to –1.75	–1.06 to 1.77	–2.10 to 2.98
Std estimate	–0.602	–0.448	–0.441	–0.475	0.059	0.042
P	<**0.0001**	<**0.0001**	**0.0005**	<**0.0001**	0.62	0.73
Sex						
Estimate	–24.04	–48.54	–14.84	–33.62	–30.02	–52.70
95% CI	–52.54 to 4.46	–76.86 to –20.22	–45.37 to 15.68	–61.46 to –5.78	–55.84 to –4.19	–99.44 to –5.96
Std estimate	–0.332	–0.693	–0.222	–0.509	–0.529	–0.533
P	0.09	**0.001**	0.33	**0.02**	**0.02**	**0.03**
APOE ε4						
Estimate	10.49	2.72	–22.41	2.24	9.98	27.86
95% CI	–17.22 to 38.19	–25.01 to 30.45	–52.02 to 7.20	–24.83 to 29.32	–15.3 to 35.26	–17.92 to 73.64
Std estimate	0.145	0.039	–0.335	0.034	0.176	0.282
P	0.45	0.85	0.14	0.87	0.43	0.23
Disease duration						
Estimate	–2.07	–0.41	–1.76	–1.41	5.36	6.97
95% CI	–5.69 to 1.55	–4.00 to 3.18	–5.69 to 2.16	–4.93 to 2.12	2.08 to 8.63	0.94 to 13.00
Std estimate	–0.114	–0.024	–0.105	–0.085	0.380	0.279
P	0.26	0.82	0.37	0.43	**0.002**	**0.02**

Six separate multivariable multiple regressions were run, one for each brain region. Age of onset and disease duration are continuous variables, expressed in years; sex is coded as male versus female and *APOE* ε4 is coded as ε4 carrier versus non-carrier. Positive estimates represent higher NFT density in patients with older age of onset, males, *APOE* ε4 carriers, and in patients with longer disease duration. CA1 = corpus ammonis sector 1. Statistically significant P-values are indicated in bold.
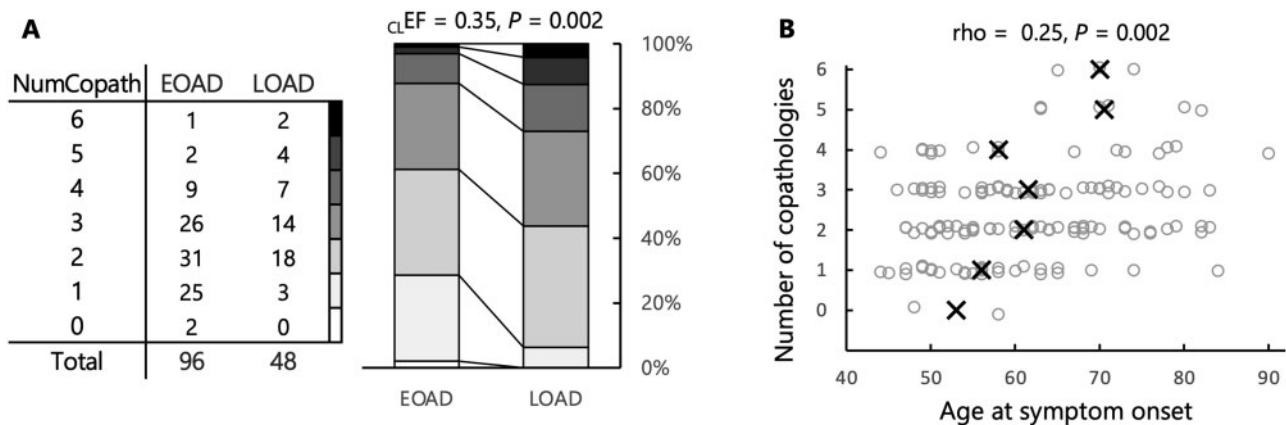

Figure 3 Number of coexistent pathologies. (**A**) The table indicates the numbers of EOAD/LOAD patients with respective total number of co-pathologies, while the stacked bars illustrate the higher number of co-pathologies in the LOAD group. Mann-Whitney U-tests were conducted to compare the two groups; common language effect size [$_{CL}EF = U / (n_{EOAD} \times n_{LOAD})$] represents the probability that a random value from the EOAD group is greater than a random value from the LOAD group. A Fisher's exact test was also run to compare the proportion of co-pathology-free cases between the two groups. (**B**) Analyses conducted with age of onset as a continuous variable. Black crosses indicate the median ages for each level of co-pathology; a random jitter was applied on the y-axis to visualize all individual data-points.

density (Table 1). In contrast, the presence of *APOE* ε4 was associated with a higher number of comorbid neuropathological diagnoses (estimate = 0.400, 95% CI 0.006 to 0.794, *P* = 0.047), independent from age at symptom onset, sex, and disease duration (Table 2). A series of exploratory logistic regression models were run to determine whether *APOE* ε4 status was associated with the presence of a specific co-pathology (all coded as present versus absent regardless of severity/stage), controlling for age of onset, sex, and disease duration. Detailed results are available in Table 3. No significant association was found between *APOE* ε4 status and CAA, α-synuclein, TDP-43, hippocampal sclerosis, vascular lesions, ATAC, or ARTAG

(P's ⩾ 0.15). A trend towards statistical significance was observed for the association with AGD (*P* = 0.09).

Influence of sex

In the overall cohort, females showed higher density of NFT compared to males, controlling for age of onset, *APOE* ε4, and disease duration. This effect was seen across all regions, and was statistically significant in the superior temporal gyrus, the angular gyrus, and hippocampal subregions CA1 and subiculum (Table 1). Complementary analyses showed that the effect of sex was not

Table 2 Independent contribution of age of onset, sex, APOE ε4, and disease duration on the number of comorbid neuropathological findings

	Estimate	SE	95% CI	Std estimate	t	P
Intercept	−1.21	0.74	−2.68 to 0.27	–	−1.62	0.11
Age of onset	0.05	0.01	0.03 to 0.06	0.374	4.48	<0.0001
Sex	−0.28	0.21	−0.69 to 0.12	−0.229	−1.38	0.17
APOE ε4	0.40	0.20	0.01 to 0.79	0.321	2.01	0.047
Disease duration	0.08	0.03	0.03 to 0.14	0.261	3.15	0.002

Full model ($n = 132$): $R^2 = 0.19$, $F(4,127) = 7.52$, $P < 0.0001$.

The number of comorbid neuropathological findings is coded as a continuous variable ranging from 0 to 6. Age of onset and disease duration are continuous variables, expressed in years; sex is coded as male versus female and APOE ε4 is coded as ε4 carrier versus non-carrier. Model showed that older age of onset, presence of the APOE ε4 allele, and longer disease duration were independently predictive of a higher number of comorbid neuropathological diagnoses.
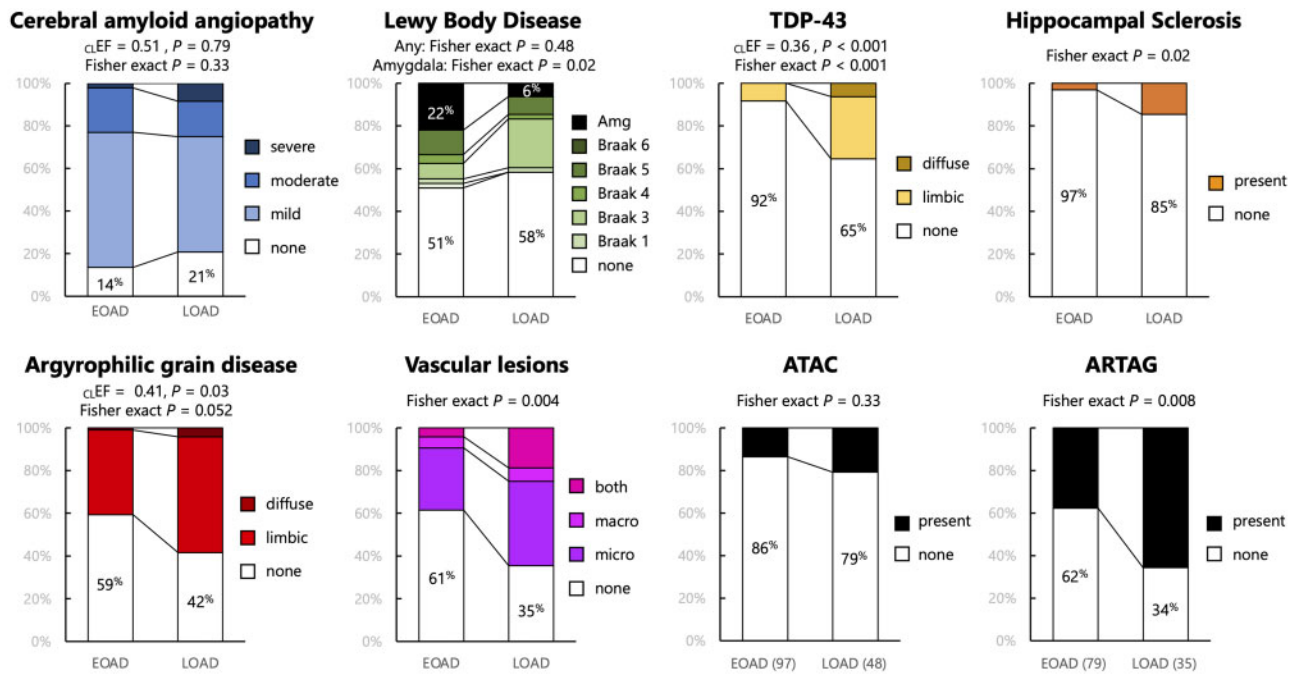

Figure 4 Details of coexistent non-Alzheimer's disease pathologies. For all co-pathologies, Fisher's exact tests were run to compare the proportion of co-pathology-free cases between the two groups. For LBD, an additional Fisher's exact test was run to compare the frequency of amygdala-predominant patterns between the two groups. For ordinal variables (TDP-43, AGD), Mann-Whitney U-tests were conducted to compare the two groups; common language effect sizes [$_{CL}EF = U / (n_{EOAD} \times n_{LOAD})$] represent the probability that a random value from the EOAD group is greater than a random value from the LOAD group. $n_{EOAD} = 96$ and $n_{LOAD} = 48$, unless otherwise specified.

modulated by age of onset (Supplementary Table 1): no sex × age group interaction was found in any region (P's ⩾ 0.17). Females consistently showed greater NFT burden than males across regions in both EOAD and LOAD subgroups, although differences were not always significant at α < 0.05 because of reduced power (Supplementary Table 3).

The effect of sex on the number of comorbid neuropathological diagnoses did not reach statistical significance (P = 0.17; Table 2). Looking at specific diagnoses, males were more likely than females to have ARTAG: 56% versus 32% (adjusted odds ratio = 2.58, 95% CI 1.09 to 6.09, P = 0.03, controlling for age of onset, APOE ε4, and disease duration; Table 3).

Analyses of cognitive and clinical decline

For both MMSE and CDR-SoB, the optimal linear fixed effect model included three main fixed effects (time until death, cohort group, and number of co-pathologies), and the interaction between time

until death and cohort group (Supplementary Tables 1 and 2 for MMSE and CDR-SoB, respectively), which were all significant (see Fig. 5B and Supplementary Fig. 3 for full description of each model).

Briefly, the MMSE model (137 patients, 382 observations, n = 40 patients have only one time point, number of available time points per patients: median = 2, min-max = 1–12, years between first and last time points: median = 1.5, min-max = 0–12.2) showed a difference between the EOAD and LOAD cohorts, with the former being more severely impaired (mean difference = 15.1, 95% CI 10.3 to 20.0) at time of death. Each additional co-pathology was associated with a decrease of 1.4 MMSE point (95% CI −2.5 to −0.2) at time of death. The time × age of onset cohort interaction was highly significant (P = 0.0001) and indicated a greater antemortem decline in MMSE in EOAD (−2.7 points/year, 95% CI −3.2 to −2.3) compared to LOAD (−1.2, 95% CI −1.8 to −0.7).

Results were similar with CDR-SoB (140 patients, 485 observations; n = 22 patients have only one time point, number of

Table 3 Relative impact of age of onset, sex, *APOE* ε4, and disease duration on the presence of each comorbid neuropathological diagnosis

	CAA	LBD, any	LBD, amygdala	TPD-43	HS	AGD	VBI	ATAC	ARTAG
n	132	132	132	132	132	132	132	132	104
Age of onset									
Estimate	–0.02	0.00	–0.08	0.10	0.09	0.04	0.10	0.03	0.05
SE	0.02	0.02	0.03	0.03	0.04	0.02	0.02	0.03	0.02
Z	–0.78	–0.27	–2.7	3.58	2.53	2.15	4.38	1.01	2.41
P	0.44	0.79	**0.007**	**0.0003**	**0.01**	**0.03**	**< 0.0001**	0.31	**0.016**
Sex									
Estimate	–0.3	0.50	0.86	–0.62	–0.76	–0.48	–0.64	1.12	0.95
SE	0.52	0.38	0.55	0.52	0.71	0.38	0.41	0.61	0.44
Z	–0.58	1.33	1.57	–1.19	–1.06	–1.25	–1.55	1.85	2.16
P	0.56	0.18	0.12	0.23	0.29	0.21	0.12	0.06	**0.03**
APOE ε4									
Estimate	0.7	0.19	–0.02	0.12	0.85	0.62	0.23	0.27	–0.03
SE	0.49	0.36	0.5	0.51	0.77	0.36	0.39	0.51	0.43
Z	1.43	0.54	–0.04	0.24	1.11	1.7	0.58	0.53	–0.08
P	0.15	0.59	0.97	0.81	0.27	0.09	0.56	0.59	0.94
Disease duration									
Estimate	–0.01	0.09	0.00	0.10	0.11	0.04	0.16	0.10	0.07
SE	0.07	0.05	0.07	0.07	0.09	0.05	0.06	0.06	0.06
Z	–0.13	1.89	0.03	1.47	1.21	0.73	2.96	1.56	1.2
P	0.90	0.06	0.98	0.14	0.23	0.47	**0.003**	0.12	0.23

Nine separate logistic regressions were run, one for each neuropathological diagnosis. Age of onset and disease duration are continuous variables, expressed in years; sex is coded as male versus female and *APOE* ε4 is coded as ε4 carrier versus non-carrier. Positive estimates (i.e. log odds) represent a higher prevalence of the neuropathological finding in patients with older age of onset, males, *APOE* ε4 carriers, and in patients with longer disease duration. SE= standard error; TDP-43= TDP-43 proteinopathy; VBI = vascular brain injury.

available time points per patient: median = 3, min-max = 1–10, years between first and last time points: median = 2.4, min-max = 0–11.5) (Supplementary Fig. 3), with the EOAD group showing higher CDR-SoB scores than the LOAD at time of death (mean difference = 5.95, 95% CI 3.41 to 8.48), and each additional co-pathology being associated with greater CDR-SoB (1.15, 95% CI 0.45 to 1.84) at death. The time × group interaction (P = 0.04) also indicated a greater premortem rate of CDR-SoB increase in EOAD (1.47 points/year, 95% CI 1.25 to 1.68) compared to LOAD (1.09, 95% CI 0.80 to 1.37).

Although none of the linear mixed effect models selected based on the lowest AIC/BIC indices included an interaction term between time and number of co-pathologies, complementary analyses showed that when these terms were forced into the models (i.e. using model 10 from Supplementary Tables 1 and 2), they were not significant: P = 0.72 for the MMSE model and P = 0.09 for the CDR-SB model.

Discussion

Frequency and severity of brain co-pathologies increase with age and contribute to the severity of the clinical phenotype in individuals with cognitive impairment.[1–3] The co-occurrence of multiple distinct neuropathological features in younger patients with dementia has been considered a rare phenomenon. Alzheimer's disease is the most common neuropathological substrate of dementia in both the older and younger populations. While the hallmark Alzheimer's disease neuropathological end-stage features of EOAD and LOAD are similar, several aspects of clinical presentation and genetic susceptibility have suggested the existence of fundamental biological differences between EOAD and LOAD that go beyond the arbitrary and simplistic age-related categorization.[44] The coexistence of distinct non-Alzheimer's disease pathologies in individuals with EOAD has so far eluded proper ascertainment because of the limited availability of large autopsy cohorts of EOAD subjects.

Our study shows the presence of one co-pathology in a quarter of patients with EOAD, two in about a third, three in more than a quarter, and four in 9% of our cohort. Our data also show an important cumulative effect of the number of coexistent non-Alzheimer's disease pathologies on clinical progression rate, a feature of both EOAD and LOAD, with no statistically significant difference between the two sexes. These data have important implications for the enrolment of EOAD subjects in longitudinal studies and clinical trials, suggesting that non-Alzheimer's disease pathological diagnoses are common and consequential, even in younger patients with Alzheimer's disease.

Coexistent LBD pathology significantly worsens the severity of the clinical presentation of Alzheimer's disease.[45] LBD pathology is frequent and clinically significant in autosomal dominant Alzheimer's disease, typically manifesting with an early age of onset.[46] Our study shows that LBD is as prevalent in sporadic EOAD as it is in LOAD, though in about a quarter of EOAD patients LBD co-pathology is predominantly confined to the amygdala. While the significance of amygdala-predominant LBD in determining the AD Alzheimer's disease clinical phenotype is likely limited,[47–49] recent observations have proposed the existence of distinctive biochemical characteristics of the amygdala-predominant α-synuclein aggregates, which may be more informative regarding the pathogenic interaction of tau and α-synuclein.[48,50,51]

Our study showed that except for CAA and LBD, the most common co-pathologies of Alzheimer's disease, namely TDP-43 proteinopathy, AGD, HS and vascular brain injury are, as expected, more common and severe in LOAD as opposed to EOAD.[1,2,27] A higher prevalence of TDP-43 pathology and HS has been described in LOAD compared to EOAD.[52] ARTAG was more commonly seen in LOAD cases compared to EOAD, as expected.[31] ATAC pathology has been associated with worse performance on neuropsychological scores in domains corresponding to the function of the anatomical area affected by this type of pathology.[53] These findings may have implications regarding the atypical, non-amnestic
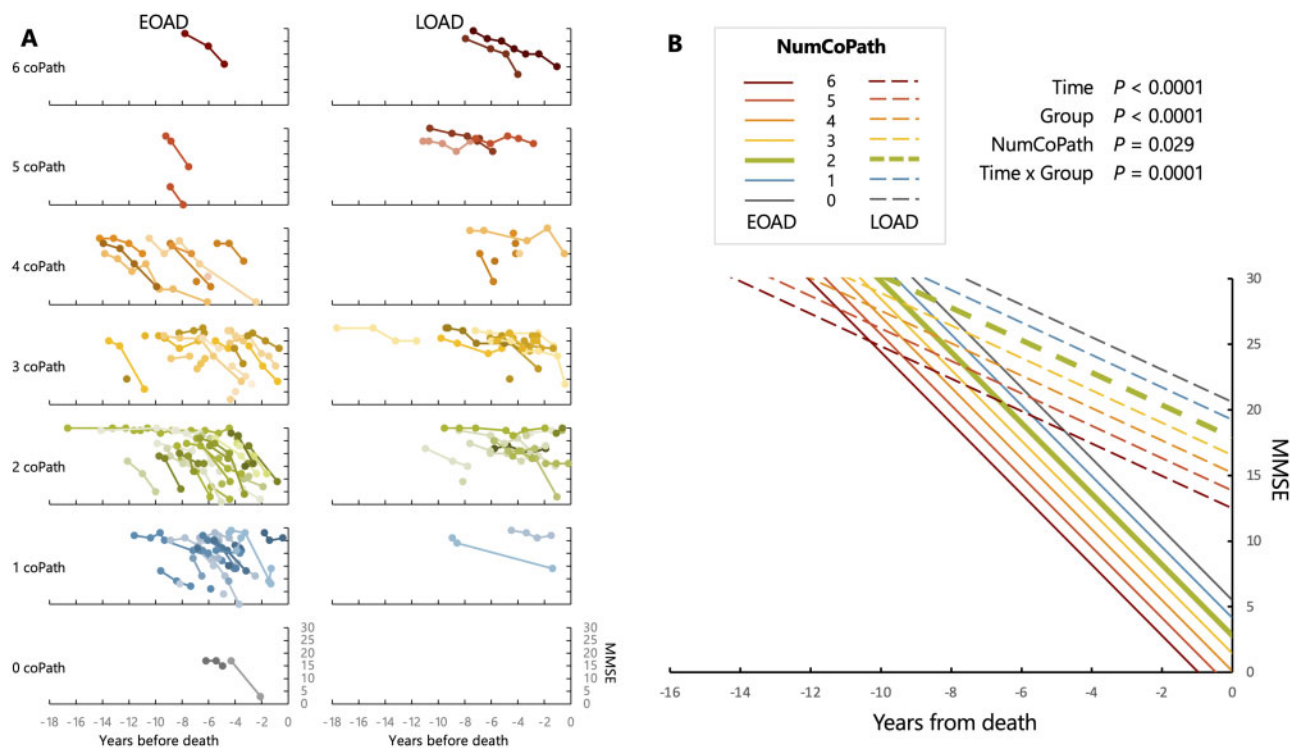
Figure 5 Antemortem cognitive decline based on MMSE. (**A**) Raw individual trajectories in MMSE scores (raw values), stratified by age of onset group (*columns*) and number of co-pathologies (*rows*). Colour variations were randomly assigned to help distinguish overlapping lines. (**B**) Results of the optimal linear mixed effect model as identified in Supplementary Table 3. The predicted MMSE trajectories for EOAD and LOAD patients with two co-pathologies (the median number of co-pathologies in the whole cohort) are emphasized by a thicker line.

clinical presentations of Alzheimer's disease, which are more commonly found in EOAD than in LOAD.[53] While in our study ATAC were more commonly found in EOAD than in LOAD, the difference did not reach statistical significance, perhaps in view of the high prevalence of non-amnestic Alzheimer's disease presentations in our LOAD cohort. Our study found a significant association between *APOE* ε4 and a higher number of co-pathologies, but no significant association between *APOE* ε4 and any of the specific pathologies, except for a trend for AGD. This is likely a consequence of the cohort size, also possibly secondary to the high prevalence in both cohorts of patients with non-amnestic Alzheimer's disease clinical presentations.[54,55]

A more rapid clinic decline has been associated with a higher severity of neuritic plaque and neurofibrillary tangles pathology in EOAD compared to LOAD.[56,57] This is consistent with recent observations based on the use of *in vivo* tau-PET demonstrating higher tau-PET signal in EOAD compared to LOAD, a difference that is significantly associated with faster rate of atrophy in EOAD compared to LOAD.[58] In our study we observed higher severity of Alzheimer's disease neuropathological hallmarks in EOAD compared to LOAD and higher rate of disease progression. In a subset of patients from the overall cohort, females showed higher density of NFT compared to males, when controlling for age of onset as a continuous variable, *APOE* ε4, and disease duration. These findings replicate previously reported observations.[59–61] There was a significantly longer survival from disease onset in EOAD compared to LOAD, a finding previously described, and possibly linked to the overall better systemic health status in the younger cohort.[62] Longer survival may, in part, allow for larger pathology burden to accumulate over time. On the other hand, differences in rate of proteinopathy accumulation have been described in various Alzheimer's disease subtypes, and are likely to play a major role in the expression of the clinical phenotype.[63]

Our study presents some limitations. While we report findings on a large autopsy series of EOAD cases, the overall cohort of Alzheimer's disease cases remains relatively small, therefore increasing the chances of occurrence of selection biases at the time of enrolment. Our autopsy cohort consists of research participants, of largely predominant white ethnicity, referred from tertiary care, academic centres and may be not reflecting of the prevalence of brain co-pathologies in a community-dwelling population. The proportion of cases with atypical, non-amnestic, Alzheimer's disease presentation is higher in our cohort than in the general population. Therefore, our findings may not be fully representative of the differences between EOAD and LOAD patients with amnestic Alzheimer's disease. Our study did not detect statistically significant differences in the effect of sex on the number of co-pathologies that have been previously described,[64] possibly as a result of the small sample size. The study of larger cohorts may help determining the effects of interactions such as the ones between *APOE* genotype and sex, age of onset, race or ethnicity. Our assessment of CAA did not include the study of capillary CAA, an important subtype of CAA associated with *APOE* ε4 carrier status with relevant effects on the pathogenesis of Alzheimer's disease.[65] Since the proportion of *APOE* ε4 carriers was similar in the EOAD and LOAD groups, it is likely that an equal representation of capillary CAA in the two groups was also present. Future studies are needed to clarify differences in the prevalence of this type of CAA across the Alzheimer's disease age spectrum. Finally, our protocol for assessing vascular brain injury is likely to underestimate the prevalence of this co-pathology.

In summary, our study shows that non-Alzheimer's disease neuropathology is common in sporadic EOAD despite a lower prevalence than in LOAD. The number of co-pathologies predicted worse cognitive performance in both cohorts. Coexistent LBD pathology was as frequent in EOAD as in LOAD, particularly in the

amygdala-predominant variant. Our findings suggest that the role of co-pathology should be considered when assessing EOAD clinical phenotype and response to treatment both in clinical practice and in clinical trials. In an era when *in vivo* PET[66–69] and plasma biomarkers[70–72] can accurately identify cases with intermediate to high Alzheimer's disease neuropathological changes with high sensitivity and specificity, it will be critical to remain mindful that additional co-pathologies, for which no robust biomarker exists today, are likely to be present even in patients with younger disease onset.

Acknowledgements

Funding

Competing interests

The authors report no competing interests.

Supplementary material

Supplementary material is available at *Brain* online.

References

1. Karanth S, Nelson PT, Katsumata Y, et al. Prevalence and clinical phenotype of quadruple misfolded proteins in older adults. *JAMA Neurol*. 2020;77:1299.
2. Robinson JL, Lee EB, Xie SX, et al. Neurodegenerative disease concomitant proteinopathies are prevalent, age-related and APOE4-associated. *Brain*. 2018;141(7):2181–2193.
3. Suemoto CK, Ferretti-Rebustini RE, Rodriguez RD, et al. Neuropathological diagnoses and clinical correlates in older adults in Brazil: A cross-sectional study. *PLoS Med*. 2017;14: e1002267.
4. Coulthard EJ, Love S. A broader view of dementia: Multiple co-pathologies are the norm. *Brain*. 2018;141(7):1894–1897.
5. Higashi S, Iseki E, Yamamoto R, et al. Concurrence of TDP-43, tau and alpha-synuclein pathology in brains of Alzheimer's disease and dementia with Lewy bodies. *Brain Res*. 2007;1184:284–294.
6. James BD, Wilson RS, Boyle PA, Trojanowski JQ, Bennett DA, Schneider JA. TDP-43 stage, mixed pathologies, and clinical Alzheimer's-type dementia. *Brain*. 2016;139(11):2983–2993.
7. McAleese KE, Walker L, Erskine D, Thomas AJ, McKeith IG, Attems J. TDP-43 pathology in Alzheimer's disease, dementia with Lewy bodies and ageing. *Brain Pathol*. 2017;27:472–479.
8. Nelson PT, Dickson DW, Trojanowski JQ, et al. Limbic-predominant age-related TDP-43 encephalopathy (LATE): consensus working group report. *Brain*. 2019;142(6):1503–1527.
9. Swirski M, Miners JS, de Silva R, et al. Evaluating the relationship between amyloid-beta and alpha-synuclein phosphorylated at Ser129 in dementia with Lewy bodies and Parkinson's disease. *Alzheimers Res Ther*. 2014;6:77.
10. Fox PJ, Phil C. Alzheimer's disease: An historical overview. *Am J Alzheimers Care Related Disord*. 1986;1:18–24.
11. Mendez MF. Early-onset Alzheimer disease and its variants. *Continuum (Minneap Minn)*. 2019;25:34–51.
12. Spina S, Brown JA, Deng J, et al. Neuropathological correlates of structural and functional imaging biomarkers in 4-repeat tauopathies. *Brain*. 2019;142(7):2068–2081.
13. Montine TJ, Phelps CH, Beach TG, et al.; Alzheimer's Association. National Institute on Aging-Alzheimer's Association guidelines for the neuropathologic assessment of Alzheimer's disease: A practical approach. *Acta Neuropathol*. 2012;123:1–11.
14. Braak H, Alafuzoff I, Arzberger T, Kretzschmar H, Del Tredici K. Staging of Alzheimer disease-associated neurofibrillary pathology using paraffin sections and immunocytochemistry. *Acta Neuropathol*. 2006;112:389–404.
15. Thal DR, Rub U, Orantes M, Braak H. Phases of A beta-deposition in the human brain and its relevance for the development of AD. *Neurology*. 2002;58:1791–1800.
16. Mirra SS, Heyman A, McKeel D, et al. The Consortium to Establish a Registry for Alzheimer's Disease (CERAD). Part II. Standardization of the neuropathologic assessment of Alzheimer's disease. *Neurology*. 1991;41:479–486.
17. Ferrer I, Santpere G, van Leeuwen FW. Argyrophilic grain disease. *Brain*. 2008;131(Pt 6):1416–1432.
18. Mackenzie IR, Neumann M, Bigio EH, et al. Nomenclature and nosology for neuropathologic subtypes of frontotemporal lobar degeneration: An update. *Acta Neuropathol*. 2010;119:1–4.
19. McKeith IG, Boeve BF, Dickson DW, et al. Diagnosis and management of dementia with Lewy bodies: Fourth consensus report of the DLB Consortium. *Neurology*. 2017;89:88–100.
20. Nelson PT, Schmitt FA, Lin Y, et al. Hippocampal sclerosis in advanced age: Clinical and pathological features. *Brain*. 2011; 134(Pt 5):1506–1518.
21. Amador-Ortiz C, Lin WL, Ahmed Z, et al. TDP-43 immunoreactivity in hippocampal sclerosis and Alzheimer's disease. *Ann Neurol*. 2007;61:435–445.
22. Banerjee G, Carare R, Cordonnier C, et al. The increasing impact of cerebral amyloid angiopathy: Essential new insights for clinical practice. *J Neurol Neurosurg Psychiatry*. 2017;88:982–994.
23. Dickson DW, Josephs KA, Amador-Ortiz C. TDP-43 in differential diagnosis of motor neuron disorders. *Acta Neuropathol*. 2007; 114:71–79.
24. Kirshner HS, Bradshaw M. The Inflammatory Form of Cerebral Amyloid Angiopathy or "Cerebral Amyloid Angiopathy-Related Inflammation" (CAARI). *Curr Neurol Neurosci Rep*. 2015;15:54.
25. McKee AC, Stern RA, Nowinski CJ, et al. The spectrum of disease in chronic traumatic encephalopathy. *Brain*. 2013;136(Pt 1):43–64.
26. Braak H, Tredici KD, Rüb U, de Vos RAI, Jansen Steur ENH, Braak E. Staging of brain pathology related to sporadic Parkinson's disease. *Neurobiol Aging*. 2003;24:197–211.
27. Rodriguez RD, Suemoto CK, Molina M, et al. Argyrophilic grain disease: Demographics, clinical, and neuropathological features from a large autopsy study. *J Neuropathol Exp Neurol*. 2016; 75:628–635.
28. Nelson PT, Smith CD, Abner EL, et al. Hippocampal sclerosis of aging, a prevalent and high-morbidity brain disease. *Acta Neuropathol*. 2013;126:161–177.
29. McAleese KE, Alafuzoff I, Charidimou A, et al. Post-mortem assessment in vascular dementia: Advances and aspirations. *BMC Med*. 2016;14:129.
30. Olichney JM, Hansen LA, Hofstetter CR, Lee JH, Katzman R, Thal LJ. Association between severe cerebral amyloid angiopathy and cerebrovascular lesions in Alzheimer disease is not a spurious one attributable to apolipoprotein E4. *Arch Neurol*. 2000;57:869–874.
31. Kovacs GG, Ferrer I, Grinberg LT, et al. Aging-related tau astrogliopathy (ARTAG): harmonized evaluation strategy. *Acta Neuropathol*. 2016;131:87–102.

32. Munoz DG, Woulfe J, Kertesz A. Argyrophilic thorny astrocyte clusters in association with Alzheimer's disease pathology in possible primary progressive aphasia. Acta Neuropathol. 2007; 114:347–357.

33. Nolan A, De Paula Franca Resende E, Petersen C, et al. Astrocytic tau deposition is frequent in typical and atypical Alzheimer disease presentations. J Neuropathol Exp Neurol. 2019; 78:1112–1123.

34. Petersen C, Nolan AL, de Paula Franca Resende E, et al. Alzheimer's disease clinical variants show distinct regional patterns of neurofibrillary tangle accumulation. Acta Neuropathol. 2019;138:597–612.

35. Armstrong MJ, Litvan I, Lang AE, et al. Criteria for the diagnosis of corticobasal degeneration. Neurology. 2013;80:496–503.

36. Crutch SJ, Schott JM, Rabinovici GD, et al.; Alzheimer's Association ISTAART Atypical Alzheimer's Disease and Associated Syndromes Professional Interest Area. Consensus classification of posterior cortical atrophy. Alzheimers Dement. 2017;13:870–884.

37. Geschwind MD. Rapidly progressive dementia. Continuum (Minneap Minn). 2016;22:510–537.

38. Gorno-Tempini ML, Hillis AE, Weintraub S, et al. Classification of primary progressive aphasia and its variants. Neurology. 2011; 76:1006–1014.

39. McKhann GM, Knopman DS, Chertkow H, et al. The diagnosis of dementia due to Alzheimer's disease: Recommendations from the National Institute on Aging-Alzheimer's Association workgroups on diagnostic guidelines for Alzheimer's disease. Alzheimers Dement. 2011;7:263–269.

40. Montenigro PH, Baugh CM, Daneshvar DH, et al. Clinical subtypes of chronic traumatic encephalopathy: Literature review and proposed research diagnostic criteria for traumatic encephalopathy syndrome. Alzheimers Res Ther. 2014;6:68.

41. Postuma RB, Berg D, Stern M, et al. MDS clinical diagnostic criteria for Parkinson's disease. Mov Disord. 2015;30:1591–1601.

42. Rascovsky K, Hodges JR, Knopman D, et al. Sensitivity of revised diagnostic criteria for the behavioural variant of frontotemporal dementia. Brain. 2011;134(Pt 9):2456–2477.

43. Perry DC, Brown JA, Possin KL, et al. Clinicopathological correlations in behavioural variant frontotemporal dementia. Brain. 2017;140(12):3329–3345.

44. Tellechea P, Pujol N, Esteve-Belloch P, et al. Early- and late-onset Alzheimer disease: Are they the same entity? Neurologia. 2018;33:244–253.

45. Malek-Ahmadi M, Beach TG, Zamrini E, et al. Faster cognitive decline in dementia due to Alzheimer disease with clinically undiagnosed Lewy body disease. PLoS One. 2019;14:e0217566.

46. Leverenz JB, Fishel MA, Peskind ER, et al. Lewy body pathology in familial Alzheimer disease: Evidence for disease- and mutation-specific pathologic phenotype. Arch Neurol. 2006;63: 370–376.

47. Roudil J, Deramecourt V, Dufournet B, et al.; and the Brainbank Neuro-CEB Neuropathology Network. Influence of Lewy pathology on Alzheimer's Disease phenotype: A retrospective clinico-pathological study. J Alzheimers Dis. 2018;63:1317–1323.

48. Sorrentino ZA, Goodwin MS, Riffe CJ, et al. Unique alpha-synuclein pathology within the amygdala in Lewy body dementia: Implications for disease initiation and progression. Acta Neuropathol Commun. 2019;7:142.

49. Uchikado H, Lin WL, DeLucia MW, Dickson DW. Alzheimer disease with amygdala Lewy bodies: A distinct form of alpha-synucleinopathy. J Neuropathol Exp Neurol. 2006;65:685–697.

50. Ferman TJ, Aoki N, Boeve BF, et al. Subtypes of dementia with Lewy bodies are associated with alpha-synuclein and tau distribution. Neurology. 2020;95:e155–e165.

51. Nelson PT, Abner EL, Patel E, et al. The amygdala as a locus of pathologic misfolding in neurodegenerative diseases. J Neuropathol Exp Neurol. 2018;77:2–20.

52. Davidson YS, Raby S, Foulds PG, et al. TDP-43 pathological changes in early onset familial and sporadic Alzheimer's disease, late onset Alzheimer's disease and Down's syndrome: Association with age, hippocampal sclerosis and clinical phenotype. Acta Neuropathol. 2011;122:703–713.

53. Resende EPF, Nolan AL, Petersen C, et al. Language and spatial dysfunction in Alzheimer disease with white matter thorn-shaped astrocytes. Neurology. 2020;94:e1353–e1364.

54. Balasa M, Gelpi E, Antonell A, et al.; For the Neurological Tissue Bank/University of Barcelona/Hospital Clinic NTB/UB/HC Collaborative Group. Clinical features and APOE genotype of pathologically proven early-onset Alzheimer disease. Neurology. 2011;76:1720–1725.

55. van der Flier WM, Pijnenburg YA, Fox NC, Scheltens P. Early-onset versus late-onset Alzheimer's disease: The case of the missing APOE varepsilon4 allele. Lancet Neurol. 2011;10:280–288.

56. Ho GJ, Hansen LA, Alford MF, et al. Age at onset is associated with disease severity in Lewy body variant and Alzheimer's disease. Neuroreport. 2002;13:1825–1828.

57. Middleton LE, Grinberg LT, Miller B, Kawas C, Yaffe K. Neuropathologic features associated with Alzheimer disease diagnosis: Age matters. Neurology. 2011;77:1737–1744.

58. La Joie R, Visani AV, Baker SL, et al. Prospective longitudinal atrophy in Alzheimer's disease correlates with the intensity and topography of baseline tau-PET. Sci Transl Med. 2020;12: eaau5732.

59. Barnes LL, Wilson RS, Bienias JL, Schneider JA, Evans DA, Bennett DA. Sex differences in the clinical manifestations of Alzheimer disease pathology. Arch Gen Psychiatry. 2005;62: 685–691.

60. Liesinger AM, Graff-Radford NR, Duara R, et al. Sex and age interact to determine clinicopathologic differences in Alzheimer's disease. Acta Neuropathol. 2018;136:873–885.

61. Oveisgharan S, Arvanitakis Z, Yu L, Farfel J, Schneider JA, Bennett DA. Sex differences in Alzheimer's disease and common neuropathologies of aging. Acta Neuropathol. 2018;136: 887–900.

62. Gronning H, Rahmani A, Gyllenborg J, Dessau RB, Hogh P. Does Alzheimer's disease with early onset progress faster than with late onset? A case-control study of clinical progression and cerebrospinal fluid biomarkers. Dement Geriatr Cogn Disord. 2012; 33:111–117.

63. Murray ME, Graff-Radford NR, Ross OA, Petersen RC, Duara R, Dickson DW. Neuropathologically defined subtypes of Alzheimer's disease with distinct clinical characteristics: A retrospective study. Lancet Neurol. 2011;10:785–796.

64. Barnes LL, Lamar M, Schneider JA. Sex differences in mixed neuropathologies in community-dwelling older adults. Brain Res. 2019;1719:11–16.

65. Thal DR, Papassotiropoulos A, Saido TC, et al. Capillary cerebral amyloid angiopathy identifies a distinct APOE epsilon4-associated subtype of sporadic Alzheimer's disease. Acta Neuropathol. 2010;120:169–183.

66. Fleisher AS, Pontecorvo MJ, Devous MD Sr, et al.; A16 Study Investigators. Positron emission tomography imaging with [18F]flortaucipir and postmortem assessment of Alzheimer disease neuropathologic changes. JAMA Neurol. 2020;77:829–839.

67. La Joie R, Ayakta N, Seeley WW, et al. Multisite study of the relationships between antemortem [(11)C]PIB-PET Centiloid values and postmortem measures of Alzheimer's disease neuropathology. Alzheimers Dement. 2019;15:205–216.

68. Lowe VJ, Lundt ES, Albertson SM, et al. Neuroimaging correlates with neuropathologic schemes in neurodegenerative disease. *Alzheimers Dement*. 2019;15:927–939.

69. Soleimani-Meigooni DN, Iaccarino L, La Joie R, et al. 18F-flortaucipir PET to autopsy comparisons in Alzheimer's disease and other neurodegenerative diseases. *Brain*. 2020;143(11):3477–3494.

70. Janelidze S, Mattsson N, Palmqvist S, et al. Plasma P-tau181 in Alzheimer's disease: Relationship to other biomarkers, differential diagnosis, neuropathology and longitudinal progression to Alzheimer's dementia. *Nat Med*. 2020;26:379–386.

71. Rodriguez JL, Karikari TK, Suarez-Calvet M, et al. Plasma p-tau181 accurately predicts Alzheimer's disease pathology at least 8 years prior to post-mortem and improves the clinical characterisation of cognitive decline. *Acta Neuropathologica*. 2020;140:267–278.

72. Thijssen EH, La Joie R, Wolf A, et al.; Advancing Research and Treatment for Frontotemporal Lobar Degeneration (ARTFL) investigators. Diagnostic value of plasma phosphorylated tau181 in Alzheimer's disease and frontotemporal lobar degeneration. *Nat Med*. 2020;26:387–397.